# Synthesis of superheavies: State of affairs and outlooks

Valery Zagrebaev[1] and Walter Greiner[2]

[1]*Flerov Laboratory of Nuclear Reactions, JINR, Dubna, Moscow Region, Russia*
[2]*Frankfurt Institute for Advanced Studies, J.W. Goethe-Universität, Frankfurt, Germany*

(Dated: October 26, 2018)

Nuclear reactions leading to formation of new superheavy elements and isotopes are discussed in the paper. "Cold" and "hot" synthesis, fusion of fission fragments, transfer reactions and reactions with radioactive ion beams are analyzed along with their abilities and limitations. Several most promising reactions are proposed for experimental study.

## I. INTRODUCTION

Two important pages in synthesis of superheavy (SH) nuclei have been overturned within last twenty years. In the "cold" fusion reactions based on the closed shell target nuclei, lead and bismuth, SH elements up to $Z = 113$ have been produced [1, 2]. The "world record" of 0.03 pb in production cross section of 113 element has been obtained here within more than half-year irradiation of $^{209}$Bi target with $^{70}$Zn beam [2]. Further advance in this direction (with Ga or Ge beams) seems to be very difficult. Note also that the SH elements obtained in the "cold" fusion reactions with Pb or Bi target are situated along the proton drip line being very neutron-deficient with a short half-life.

The cross sections for SH element production in more asymmetric (and "hoter") fusion reactions of $^{48}$Ca with actinide targets were found much larger [3]. Even 118 element was produced with the cross section of about 1 pb in the $^{48}$Ca+$^{249}$Cf fusion reaction [4]. Fusion of actinides with $^{48}$Ca leads to more neutron-rich SH nuclei with much longer half-lives. However they are still far from the center of the predicted "island of stability" formed by the neutron shell around $N = 184$ (these are the $^{48}$Ca induced fusion reactions which confirm an existence of this "island of stability"). Moreover, californium is the heaviest actinide which can be used as a target material in this method (the half-life of the most long-living einsteinium isotope, $^{252}_{99}$Es, is 470 days, sufficient to be used as target material, but it is impossible to accumulate required amount of this matter).

In this connection other ways for the production of SH elements with $Z > 118$ and also neutron rich isotopes of SH nuclei in the region of the "island of stability" should be searched for. In this paper we analyze abilities and limitations of different nuclear reactions leading to formation of SH elements ("cold" and "hot" synthesis, symmetric fusion, transfer reactions and reactions with radioactive beams) trying to find most promising reactions which may be used at available facilities.

## II. THE MODEL

The cross section of SH element production in heavy ion fusion reaction (with subsequent evaporation of $x$ neutrons in the cooling process) is calculated as follows

$$\sigma_{\mathrm{ER}}^{\mathrm{xn}}(E) = \frac{\pi}{k^2} \sum_{l=0}^{\infty} (2l+1) P_{\mathrm{cont}}(E,l) \cdot P_{\mathrm{CN}}(E^*,l) \cdot P_{\mathrm{xn}}(E^*,l).$$
(1)

Empirical or quantum channel coupling models [5] may be used to calculate rather accurately penetrability of the multi-dimensional Coulomb barrier $P_{\mathrm{cont}}(E,l)$ and the corresponding capture (sticking) cross section, $\sigma_{\mathrm{cap}}(E) = \pi/k^2 \sum (2l+1) P_{\mathrm{cont}}$. The survival probability $P_{\mathrm{xn}}(E^*)$ of an excited compound nucleus (CN) can be calculated within a statistical model. We use here the fission barriers and other properties of SH nuclei predicted by the macro-microscopic model [6]. Other parameters determining the decay widths and the algorithm itself for a calculation of the light particle evaporation cascade and $\gamma$ emission are taken from [7]. All the decay widths may be easily calculated also at the Web site [5].

The probability for compound nucleus formation $P_{\mathrm{CN}}(E,l)$ is the most difficult part of the calculation. In [8] the two-dimensional master equation was used for estimation of this quantity, and a strong energy dependence of $P_{\mathrm{CN}}$ was found, which was confirmed recently in experiment [9]. Later the multi-dimensional Langevin-type dynamical equations were proposed [10, 11] for the calculation of the probability for CN formation both in "cold" and "hot" fusion reactions. The main idea is to study evolution of the heavy nuclear system driven by the time dependent multi-dimensional potential energy surface gradually transformed to the adiabatic potential calculated within the two-center shell-model [12]. Note that the extended version of this model developed recently in [13] leads to a correct asymptotic value of the potential energy of two separated nuclei and height of the Coulomb barrier in the entrance channel (fusion), and appropriate behavior in the exit channel, giving the required mass and energy distributions of reaction products and fission fragments.

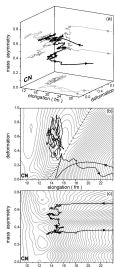In the case of near-barrier collision of heavy nuclei only

FIG. 2: Survival probability $P_{xn}(E^*, l = 0)$ of $^{256}$No, $^{258}$Rf and $^{262}$Sg compound nuclei produced in the $^{48}$Ca+$^{208}$Pb, $^{50}$Ti+$^{208}$Pb and $^{54}$Cr+$^{208}$Pb fusion reactions. The arrows indicate the Bass barriers (see Table I).

receiving rather reliable estimations of the reaction cross sections discussed below. Such estimations are urgently needed for planning future experiments in this field.

## III.   COLD FUSION REACTIONS

At near-barrier incident energies fusion of heavy nuclei ($^{48}$Ca, $^{50}$Ti, $^{54}$Cr and so on) with $^{208}$Pb or $^{209}$Bi targets leads to formation of low-excited superheavy CN ("cold" synthesis). In spite of this favorable fact (only one or two neutrons are to be evaporated), the yield of evaporation residues sharply decreases with increasing charge of synthesized SH nucleus. There are two reasons for that. First, in these reactions neutron deficient SH nuclei are produced far from the closed shells or sub-shells. As a result, neutron separation energies of these nuclei are rather high whereas the fission barriers (macroscopic components plus shell corrections) are rather low (see Table I). This leads to low survival probability even for 1n and 2n evaporation channels, Fig. 2.

TABLE I: Fission barriers (macroscopical part and shell correction) and neutron separation energies (MeV) of CN produced in the $^{48}$Ca+$^{208}$Pb, $^{50}$Ti+$^{208}$Pb and $^{54}$Cr+$^{208}$Pb fusion reactions [6]. The last column shows the excitations of CN at the Bass barrier [16] incident energies.

| CN | $B_{LD}$ | Sh.Corr. | $B_{fis}$ | $E_n^{sep}$ | $E^*$(Bass) |
|---|---|---|---|---|---|
| $^{256}$No | 1.26 | 4.48 | 5.7 | 7.1 | 22 |
| $^{258}$Rf | 0.71 | 4.49 | 5.3 | 7.6 | 24 |
| $^{262}$Sg | 0.47 | 4.63 | 5.1 | 7.8 | 24 |

The main reason for low yields of evaporation residues in these reactions is, however, a sharp decrease of the fusion probability with increasing charge of the projectile. In Fig. 3 the calculated capture, CN formation and evaporation residue (EvR) cross sections of the $^{208}$Pb induced fusion reactions are shown along with available



FIG. 1: Collision of $^{48}$Ca +$^{248}$Cm at $E_{c.m.} = 210$ MeV. One of typical trajectories calculated within the Langevin equations and going to the quasi-fission exit channel (lead valley) is shown in the three-dimensional space (a) and projected onto the "deformation–elongation" (b) and "mass-asymmetry–elongation" (c) planes. The dashed line in (b) shows the ridge of the multidimensional Coulomb barrier.

a few trajectories (of many thousands tested) reach the CN configuration (small values of elongation and deformation parameters, see Fig. 1). All others go out to the dominating deep inelastic and/or quasi-fission exit channels. One of such trajectories is shown in Fig. 1 in the three-dimensional space of "elongation–deformation–mass-asymmetry" used in the calculations.

Made within our approach the predictions for the excitation functions of SH element production with Z=112÷118 in 1n÷5n evaporation channels of the $^{48}$Ca induced fusion reactions [14, 15] agree well with the later obtained experimental data. This gives us confidence in
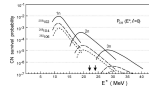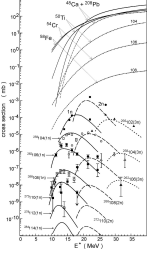
FIG. 4: Calculated fusion probabilities, $P_{\mathrm{CN}}(E^*, l = 0)$, for near-barrier collisions of heavy nuclei with $^{208}$Pb target. CN excitation energies at the Bass barriers are shown by the arrows. Experimental values of $P_{\mathrm{CN}}$ obtained in [9] for the $^{50}$Ti+$^{208}$Pb fusion reaction are shown by the rectangles.

by the simple formula

$$P_{\mathrm{CN}}(E^*, l) = \frac{P_{\mathrm{CN}}^0}{1 + exp[\dfrac{E_{\mathrm{B}}^* - E_{\mathrm{int}}^*(l)}{\Delta}]}, \qquad (2)$$

which could be useful for a fast estimation of EvR cross sections in the "cold" fusion reactions. Here $E_{\mathrm{B}}^*$ is the excitation energy of CN at the center-of-mass beam energy equal to the Bass barrier [16]. $E_{\mathrm{B}}^*$ are shown in Fig. 4 by the arrows. $E_{\mathrm{int}}^*(l) = E_{\mathrm{c.m.}} + Q - E_{\mathrm{rot}}(l)$ is the "internal" excitation energy which defines also the damping of the shell correction to the fission barrier of CN. $\Delta$ is the adjustable parameter of about 4 MeV, and $P_{\mathrm{CN}}^0$ is the "asymptotic" (above-barrier) fusion probability dependent only on a combination of colliding nuclei.

The values of $P_{\mathrm{CN}}^0$ calculated at excitation energy $E^* = 40$ MeV (well above the barriers for the "cold" fusion reactions) demonstrate rather simple behavior (almost linear in logarithmic scale), monotonically decreasing with increase of charge of CN and/or with increase of the product of $Z_1$ and $Z_2$, see Fig. 5. This behavior could be also approximated by very simple Fermi function

$$P_{\mathrm{CN}}^0 = \frac{1}{1 + exp[\dfrac{Z_1 Z_2 - \zeta}{\tau}]}, \qquad (3)$$

where $\zeta \approx 1760$ and $\tau \approx 45$ are just the fitted parameters. Eq.(3) is obviously valid only for the "cold" fusion reactions of heavy nuclei with the closed shell targets $^{208}$Pb and $^{209}$Bi. Unfortunately we have not enough experimental data to check this formula for other reactions (or to derive more general expression for the fusion probability).

Two important remarks could be done after our analysis of the "cold" fusion reactions. The first is rather evi-



FIG. 3: Capture (upper solid curves), CN formation (short-dashed curves) and SH element production cross sections in the $^{208}$Pb induced fusion reactions. 1n, 2n and 3n evaporation channels are shown by solid, dashed and dotted curves (theory) and by rectangles, circles and triangles (experiment), correspondingly. Experimental data are taken from [1, 2, 17].

experimental data on the yields of SH elements (not all experimental points are displayed to simplify the plot). The fusion probabilities $P_{\mathrm{CN}}$, calculated for head-on collisions (which bring the main contribution to the EvR cross sections), demonstrate a sharp energy dependence (see Fig. 4), found earlier in [8]. Recently the decrease of the fusion probability at subbarrier energies was confirmed experimentally for the fusion of $^{50}$Ti with $^{208}$Pb [9].

We found that the calculated energy dependence of the fusion probability (shown in Fig. 4) may be approximated
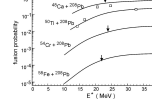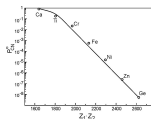
FIG. 5: Above-barrier CN formation probability in the $^{208}$Pb induced fusion reactions. Results of calculation are shown by the circles, whereas the fitted curve corresponds to the expression (3).

dent. There are no reasons (in fusion or in survival probabilities) to slow down the fast monotonic decrease of EvR cross sections with increasing charge of SH nucleus synthesized in the "cold" fusion reaction. The yield of 114 element in the 1n evaporation channel of the $^{76}$Ge+$^{208}$Pb fusion reaction is only 0.06 pb. For 116 and 118 elements, synthesized in fusion reactions of $^{82}$Se and $^{86}$Kr with lead target, we found only 0.004 pb and 0.0005 pb, correspondingly, for 1n EvR cross sections (it is worth to note that our results disagree with those obtained within the "concept of the dinuclear system" [18], which predicts the EvR cross sections at the level of 0.1 pb for all these elements including Z=120). As already mentioned, fusion reactions with $^{208}$Pb or $^{209}$Bi targets lead to neutron deficient SH nuclei with short half-lives, that may bring an additional difficulty to their experimental detection at the available separators.

The second conclusion is important for further experiments with actinide targets. The experimental value of EvR cross section for 104 element in the $^{50}$Ti+$^{208}$Pb fusion reaction is two orders of magnitude less as compared with the yield of 102 element in the $^{48}$Ca+$^{208}$Pb reaction, see Fig. 3. At first sight, this fact makes the fusion reactions of titanium with actinide targets ("hot" fusion) much less encouraging as compared to $^{48}$Ca fusion reactions. However, this sharp decrease in the yield of the Rutherfordium isotopes is caused by the two reasons. One order of magnitude loss in the EvR cross section is due to the low survival probability of $^{258}$Rf nucleus (the fission barrier is less by 0.4 MeV and neutron separation energy is higher by 0.5 Mev as compared with $^{256}$No, Fig. 2), whereas the fusion probability of $^{50}$Ti with $^{208}$Pb at energies near and above the Coulomb barrier is only one order of magnitude less than in the $^{48}$Ca+$^{208}$Pb fusion reaction (see Fig. 4). This makes titanium beam

quite promising for synthesis of SH nuclei in fusion reactions with the actinide targets (see below).

## IV. HOT FUSION REACTIONS

Fusion reactions of $^{48}$Ca with actinide targets lead to formation of more neutron rich SH nuclei as compared to the "cold" fusion reactions. Their half-lives are several orders of magnitude longer. For example, the half-life of the SH nucleus $^{277}$112 synthesized in the "cold" fusion reaction $^{70}$Zn+$^{208}$Pb [1, 2] is about 1 ms, whereas $T_{1/2}(^{285}112) \sim 34$ s [3] (approaching the "island of stability"). On average, these SH nuclei have higher fission barriers and lower neutron separation energies, which give them a chance to survive in the neutron evaporation cascade.

Unfortunately, weaker binding energies of the actinide nuclei lead to rather high excitation energies of obtained CN (that is why these reactions are named "hot"). At beam energy close to the Bass barrier the value of $E_{\mathrm{CN}}^* = E_{\mathrm{c.m.}} + B(Z_{\mathrm{CN}}, A_{\mathrm{CN}}) - B(Z_1, A_1) - B(Z_2, A_2)$ ($B$ is the binding energy) is usually higher than 30 MeV for almost all the combinations, and at least 3 neutrons are to be evaporated to get a SH nucleus in its ground state. The total survival probability of CN formed in the "hot" fusion reaction (in the 3n and/or in the 4n channel) is much less than 1n-survival probability in the "cold" fusion reaction, $P_{\mathrm{3n}}^{\text{"hot"}}(E^* \sim 35\,\mathrm{MeV}) << P_{\mathrm{1n}}^{\text{"cold"}}(E^* \sim 15\,\mathrm{MeV})$.

On the other hand, for the more asymmetric "hot" combinations the fusion probability is usually much higher as compared to the "cold" combinations leading to the same (but more neutron deficient) elements. We calculated the capture, fusion and EvR cross sections for the "cold" ($^{208}$Pb induced) and "hot" ($^{48}$Ca induced) reactions leading to SH nuclei with $Z = 102 \div 118$ at the same excitation energies of the CN – 15 MeV for the "cold" and 35 MeV for the "hot" combinations. Of course, the beam energies, at which these CN excitations arise, are equal only approximately to the corresponding Coulomb barriers and not all them agree precisely with positions of maxima of EvR cross sections. However, some general regularities can be found from these calculations.

The results of our calculations are shown in Fig. 6. As can be seen, the capture cross sections are about one order of magnitude larger for the "hot" combinations. This is because the $E^* = 15$ MeV corresponds to the incident energies somewhat below the Bass barriers of the "cold" combinations. Slow decrease of $\sigma_{\mathrm{cap}}$ for the "cold" combinations at $Z_{\mathrm{CN}} > 108$ is caused by gradual shallowing of the potential pocket (decreasing value of $l_{\mathrm{crit}}$). Larger value of $\sigma_{\mathrm{cap}}$ for the $^{48}$Ca+$^{249}$Cf combination is conditioned by a "colder" character of this reaction – the excitation energy of CN at the Bass barrier beam energy is only 28 MeV for this reaction (i.e., $E^* = 35$ MeV corresponds here to above barrier initial energy).

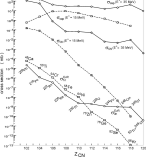The fusion probability for the "cold" combinations decreases very fast with increasing charge of the projec-

ements 102 ($^{208}$Pb target) and 112 ($^{238}$U target). For deeper understanding of the mechanisms of SH element formation, an additional point in this region (where the cross section falls down by four orders of magnitude) is extremely desirable. We found that the neutron rich isotopes of Hassium (Z=108) could be produced in the $^{48}$Ca+$^{226}$Ra fusion reaction with rather large cross sections, Fig. 7. In such experiment one should worry about utilization of $^{222}$Rn (decaying finally to rather long-lived $^{210}$Po), however, $^{226}$Ra target was already used in the past. Simultaneous measurement of the capture cross section could be also rather useful for subsequent theoretical analysis. Note, that our estimation of the EvR cross sections in this reaction is rather close to those obtained in [19].
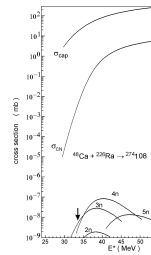


FIG. 6: Calculated capture, fusion and evaporation residue cross sections in the "cold" $^{208}$Pb induced (rectangles joined by dashed lines, projectiles are shown) and "hot" $^{48}$Ca induced (circles joined by solid lines, targets are shown) fusion reactions. The cross sections are calculated at beam energies corresponding to 15 MeV ("cold" fusion, 1n channel) and 35 MeV ("hot" fusion, 3n channel) excitation energies of the compound nuclei.

tile and, in spite of evaporation of only one neutron, at $Z_{\rm CN} \geq 112$ the EvR cross sections become less than in "hot" fusion reactions. Increasing survival probability of SH nuclei with $Z = 114, 116$ synthesized in $^{48}$Ca induced fusion reactions as compared to $Z = 110, 112$ is due to the increase of the shell corrections to the fission barriers of these nuclei caused by approaching the closed shells predicted by the macro-microscopical model (see Table II).

TABLE II: Fission barriers (macroscopical part and shell correction) and neutron separation energies (MeV) of CN produced in the $^{48}$Ca fusion reactions with $^{232}$Th, $^{238}$U, $^{244}$Pu, $^{248}$Cm and $^{249}$Cf targets [6]. The last column shows the excitations of CN at the Bass barrier incident energies.

| CN | $B_{\rm LD}$ | Sh.Corr. | $B_{\rm fis}$ | $E_n^{\rm sep}$ | $E^*$(Bass) |
|---|---|---|---|---|---|
| $^{280}$110 | 0.21 | 4.76 | 5.0 | 7.0 | 32 |
| $^{286}$112 | 0.10 | 6.64 | 6.7 | 7.1 | 33 |
| $^{292}$114 | 0.04 | 8.89 | 8.9 | 7.0 | 34 |
| $^{296}$116 | 0.01 | 8.58 | 8.6 | 6.7 | 32 |
| $^{297}$118 | 0.00 | 8.27 | 8.3 | 6.2 | 28 |

In the experimental data on the "hot" fusion reactions induced by $^{48}$Ca there is unexplored gap between the el-



FIG. 7: Calculated capture, fusion and evaporation residue (2n, 3n, 4n and 5n channels) cross sections in the $^{48}$Ca+$^{226}$Ra fusion reaction. The arrow indicates the Bass barrier.

In the series of SH elements synthesized in the $^{48}$Ca induced fusion reactions [3] one element, Z=117, is still "skipped". The element 117 may be synthesized with
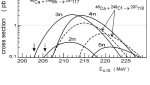
FIG. 8: Cross sections for production of the element 117 in the $^{48}$Ca+$^{249}$Bk fusion reaction (solid curves, 2n, 3n, 4n and 5n evaporation channels). For comparison the EvR cross sections in 3n and 4n channels of the $^{48}$Ca+$^{249}$Cf fusion reaction are shown by the dashed curves. The arrows indicate the corresponding Bass barriers.

rather large cross section in the $^{48}$Ca+$^{249}$Bk fusion reaction, if one manages to prepare a short-living (330 days) berkelium target. The calculated EvR cross sections of this reaction are shown in Fig. 8. It is important that the successive nuclei ($^{289,290}$115, $^{285,286}$113, $^{281,282}$111, $^{277,278}$109, and so on) appearing in the $\alpha$-decay chains of $^{293,294}$117 are assumed to have rather long half-lives to be detected and studied in the chemical experiment, that makes the $^{48}$Ca+$^{249}$Bk fusion reaction quite attractive. Also the berkelium target may be used for synthesis of the element 119 in fusion reaction with the titanium beam (see below).

As mentioned above, $^{249}$Cf ($T_{1/2} = 351$ y) is the heaviest available target which may be used in experiment. Thus, to get SH elements with $Z > 118$ in fusion reactions we should proceed to heavier than $^{48}$Ca projectiles. Most neutron-rich isotopes of 120-th element may be synthesized in the three different fusion reactions $^{54}$Cr+$^{248}$Cm, $^{58}$Fe+$^{244}$Pu and $^{64}$Ni+$^{238}$U leading to the same SH nucleus $^{302}$120 with neutron number near to the predicted closed shell N=184. These three combinations are not of equal worth. In Fig. 9 the potential energy surface for the nuclear system consisting of 120 protons and 182 neutrons is shown in the "elongation–mass-asymmetry" space at fixed value of dynamic deformation $\beta_2 = 0.2$. One can see that the contact configuration of the more symmetric $^{64}$Ni+$^{238}$U combination is located lower in the valley leading the nuclear system to the dominating quasi-fission channels.

As a result the estimated EvR cross sections for more symmetric $^{58}$Fe+$^{244}$Pu and $^{64}$Ni+$^{238}$U reactions are lower as compared to the less symmetric $^{54}$Cr+$^{248}$Cm combination (see Fig. 10). Some gain for $^{64}$Ni+$^{238}$U comes from the "colder" character of this reaction – the excitation of CN at the Bass barrier incident energy for this combination, $E^*_{CN} = 26$ MeV, is much lower than for two others (see arrows in Fig. 10). Note, that 3n and 4n evaporation residues of the $^{302}$120 nucleus will decay
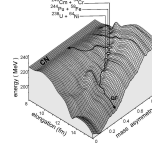


FIG. 9: Potential energy surface for the nuclear system consisting of 120 protons and 182 neutrons (elongation–mass-asymmetry plot at fixed dynamic deformation $\beta_2 = 0.2$). Injection configurations (contact points) for the $^{54}$Cr+$^{248}$Cm, $^{58}$Fe+$^{244}$Pu and $^{64}$Ni+$^{238}$U fusion reactions are shown by the circles. Thick curves with arrows shows schematically quasi-fission and fusion (CN formation) trajectories.

over the known isotopes of $112 \div 118$ elements [3]. This significantly simplifies their identification. However, the $Q$-value of the first $\alpha$-particle emitted from the element 120 should be rather high (about 13 MeV) and the half-life of this element might be rather short. If it is comparable with the time of flight of the recoil nucleus through a separator (about 1 $\mu s$), then an additional difficulty appears in detection of this element.
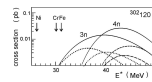


FIG. 10: Excitation functions for production of the Z=120 element in 3n and 4n evaporation channels of the $^{54}$Cr+$^{248}$Cm (solid curves), $^{58}$Fe+$^{244}$Pu (dashed) and $^{64}$Ni+$^{238}$U (dotted) fusion reactions. The corresponding Bass barriers are shown by the arrows.

When calculating survival probability we used the fission barriers of SH nuclei predicted by the macro-microscopical model [6], which gives much lower fission

barrier for $^{302}120$ nucleus as compared to $^{296}116$. On the other hand, the full microscopic models based on the self-consistent Hartree–Fock calculations [20] predict much higher fission barriers for the nucleus $^{302}120$ (up to 10 MeV) if the Skyrme forces are used (though these predictions are not unambiguous and depend strongly on chosen nucleon-nucleon forces). This means that the estimated 3n and 4n EvR cross sections in the fusion reactions considered above could be, in principle, higher than those shown in Fig. 10. This fact, however, influences neither the positions of the maxima of the excitation functions nor the conclusion about the advantage of the $^{54}$Cr+$^{248}$Cm fusion reaction as compared to $^{64}$Ni+$^{238}$U.

Strong dependence of the calculated EvR cross sections for the production of 120 element on mass-asymmetry in the entrance channel (along with their low values for all the reactions considered above) makes the nearest to $^{48}$Ca projectile, $^{50}$Ti, most promising for further synthesis of SH nuclei. Of course, the use of the titanium beam instead of $^{48}$Ca also decreases the yield of SH nuclei mainly due to a worse fusion probability. The calculated excitation functions for synthesis of 116, 117, 119 and 120 SH elements in the fusion reactions of $^{50}$Ti with $^{244}$Pu, $^{243}$Am, $^{249}$Bk and $^{249}$Cf targets are shown in Fig. 11.

The orientation effects are known to play an important role in fusion reactions of statically deformed heavy nuclei [11, 14, 15]. The fusion probability (formation of CN) was found to be strongly suppressed for more elongated nose-to-nose initial orientations [11]. As a result the preferable beam energies for synthesis of SH elements in the "hot" fusion reactions are shifted to values which are several MeV higher then the corresponding Bass barriers (calculated for spherical nuclei). As can be seen from Fig. 11, the estimated EvR cross sections for 117, 119 and 120 SH elements synthesized in the $^{50}$Ti induced reactions are quite reachable at available experimental setups, though one needs longer time of irradiation as compared with $^{48}$Ca fusion reactions.

## V. MASS SYMMETRIC FUSION REACTIONS

The use of the accelerated neutron-rich fission fragments is one of the widely discussed speculative methods for the production of SH elements in the region of the "island of stability". For example, in the $^{132}$Sn+$^{176}$Yb fusion reaction we may synthesize $^{308}120$, which (after a few neutron evaporations and $\alpha$-decays) may reach a center of the "island of stability". Several projects in the world are now realizing to get the beams of neutron rich fission fragments. The question is how intensive should be such beams to produce SH nuclei. Evidently the answer depends on the values of the corresponding cross sections. Unfortunately, there are almost no experimental data on fusion reactions in mass-symmetric nuclear combinations.

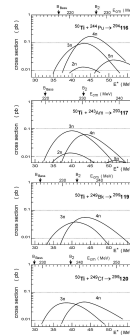Experimental data on symmetric fusion reactions



FIG. 11: Excitation functions of $^{50}$Ti induced synthesis of 116, 117, 119 and 120 elements. The arrows indicate the positions of the corresponding Bass barriers and the Coulomb barriers of side-by-side oriented nuclei.

$^{100}$Mo+$^{100}$Mo, $^{100}$Mo+$^{110}$Pa and $^{110}$Pa+$^{110}$Pa [21] show that the fusion probability sharply decreases with increasing mass and charge of colliding nuclei. However, the last studied reactions of such kind, $^{110}$Pa+$^{110}$Pa, is still far from a combination leading to a SH compound nucleus. This means that further experimental study of

such reactions is quite urgent.

The choice of the colliding nuclei is also important. In this connection the $^{136}$Xe+$^{136}$Xe fusion reaction looks very promising for experimental study [22], because the formed CN, $^{272}$Hs, should undergo just to symmetric fission. It means that two colliding $^{136}$Xe nuclei are very close to the nascent fission fragments of $^{272}$Hs in the region of the saddle point, and their fusion should really reflect a fusion process of two fission fragments.
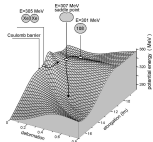


FIG. 13: Evaporation residue cross sections in the $^{136}$Xe+$^{136}$Xe fusion reactions. Solid lines show our predictions [24], whereas the dashed curves are the predictions taken from Ref. [25]. Gray bar shows upper limit of the experimental EvR cross sections in this reaction [27].



FIG. 12: Adiabatic potential energy of the $^{272}$108 nuclear system at zero mass asymmetry ($^{136}$Xe+$^{136}$Xe configuration in asymptotic region) in the "elongation–deformation" space. The curves with arrows show the fission and fusion paths. The circles show positions of CN, saddle point and contact configuration of two spherical Xe nuclei.

The calculated within the two-center shell model adiabatic potential energy surface of the nuclear system consisting of 108 protons and 164 neutrons is shown in Fig. 12 as a function of elongation (distance between the centers) and deformation of the fragments at zero mass asymmetry, which correspond to two Xe nuclei in the entrance and exit channel. The energy scale is chosen in such a way that zero energy corresponds to two $^{136}$Xe nuclei in their ground states at infinite distance. The contact configuration of two spherical Xe nuclei is located very close (in energy and in configuration space) to the saddle point of CN (note that it is located behind the Coulomb barrier, though there is no pronounced potential pocket). This fusion reaction is extremely "cold", the excitation energy of the CN at the Bass barrier beam energy is only 5 MeV. One may expect that after contact these nuclei may overcome the inner barrier due to fluctuations of collective degrees of freedom and thus reach the saddle configuration. After that they fuse (form CN) with 50% probability.

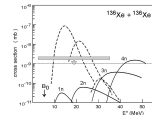However the potential energy decreases very fast with increasing deformations of the touching nuclei and drives the nuclear system to the fission valley (see Fig. 12). As a result, the calculated fusion probability is very low and, in spite of rather high fission barriers of the hassium isotopes in the region of $A \sim 270$ ($\sim 6$ MeV [6]), the EvR cross sections were found to be very low [24], see Fig. 13. They are much less than the yield of $^{265}$Hs synthesized in the more asymmetric $^{58}$Fe+$^{208}$Pb fusion reaction (Fig. 3). It is worthy to note that the prediction of the EvR cross section for the 1n channel in the $^{136}$Xe+$^{136}$Xe fusion reaction, obtained within the so-called "diffusion model" [26], exceeds our result by three orders of magnitude. This fact reflects significant difficulties appearing in the calculation of the fusion probability in such reactions.

Experiment on the synthesis of hassium isotopes in the $^{136}$Xe+$^{136}$Xe fusion reaction was performed recently in Dubna, and no one event was detected at the level of about 2 pb [27]. Thus, we may conclude that for the widely discussed future experiments on synthesis of SH nuclei in the fusion reactions with accelerated fission fragments one needs to get a beam intensity not lower than $10^{13}$ pps (comparable or greater than intensities of available stable beams of heavy ions). Since the experimental values of the EvR cross sections in such reactions are still unknown, attempts to synthesize a SH element in the fusion reaction of two heavy more or less equal in masses nuclei (Xe+Xe or Sn+Xe) should be continued.

## VI. RADIOACTIVE ION BEAMS

Recently many speculations also appeared on the use of radioactive beams for synthesis and study of new ele-

ments and isotopes. A rather complete list of references as well as a review on this problem can be found in the paper of Loveland [28].

As shown above, the use of accelerated fission fragments for the production of SH nuclei in symmetric fusion reactions is less encouraging and needs beam intensities at the hardly reachable level of $10^{13}$ pps or higher. In our opinion, they are the lighter radioactive beams which could be quite useful to solve the two important problems. As can be seen from Fig. 14 there is some gap between the SH nuclei produced in the "hot" fusion reactions with $^{48}$Ca and the mainland. This gap hinders obtaining a clear view on the properties of SH nuclei in this region (in particular, positions of closed shells and sub-shells). There are no combinations of stable nuclei to fill this gap in fusion reactions, while the use of radioactive projectiles may help to do this.
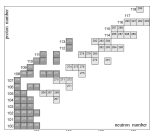
Contrary to a common opinion, neutron excess itself does not increase very much the EvR cross sections in fusion reactions of neutron rich radioactive nuclei. The neutron excess decreases just a little the height of the Coulomb barrier due to the small increase in the radius of neutron rich projectile. Neutron transfer with positive $Q$-value may really increase the sub-barrier fusion probability by several orders of magnitude due to "sequential fusion mechanism" [29, 30]. However, this mechanism does not increase noticeably the fusion probability at near-barrier incident energies, where the EvR cross sections are maximal (see above).

Fig. 15 shows the EvR cross sections for the $^{44}$S+$^{248}$Cm fusion reaction, in which the isotopes of the element 112 with six more neutrons (as compared with the $^{48}$Ca+$^{238}$U reaction) could be synthesized. The calculated one-picobarn cross sections mean that the beam intensity of sulfur-44 (which may be produced, for example, by 4p stripping from $^{48}$Ca) should be no less than $10^{12}$ pps to synthesize these extremely neutron rich isotopes.
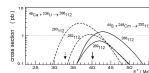


FIG. 14: Upper part of the nuclear map. Isotopes synthesised in the $^{48}$Ca induced fusion reactions are shown by the light gray rectangles.



FIG. 15: Excitation functions for the synthesis of the isotopes of the element 112 in 3n and 4n evaporation channels of the $^{48}$Ca+$^{238}$U (A=282 and A=283, dashed curves) and $^{44}$S+$^{248}$Cm (A=288 and A=289, solid curves) fusion reactions. Arrows indicate the corresponding Bass barriers for the two reactions.

The second problem, which may be solved with the radioactive beams, is obtaining much more neutron rich transfermium isotopes. It is extremely important for two reasons. First, as we know from experiment, the addition of only 8 neutrons to nucleus $^{277}$112($T_{1/2}$ = 0.7 ms) increases its half-life by almost 5 orders of magnitude – $T_{1/2}(^{285}$112$)$ = 34 s – testifying the approach of the "island of stability". How far is it? How long could be half-lives of SH nuclei at this island? To answer these questions we need to add more and more neutrons. Second, somewhere in the region of Z∼100 and N∼170 the r-process of nucleosynthesis should be terminated by neutron-induced or $\beta$-delayed fission. This region of nuclei, however, is absolutely unknown and only theoretical estimations of nuclear properties (rather unreliable for neutron rich isotopes) are presently used in different astrophysical scenarios.

In utmost mass-asymmetric fusion reactions (with lighter than neon projectiles) there is no suppression of CN formation: after contact colliding nuclei form CN with almost unit probability, $P_{CN} \approx 1$. This significantly increases the EvR cross sections in such reactions and, in spite of the rather difficult production of light radioactive nuclei with significant neutron excess, they could be used for the study of neutron rich transfermium nuclei.

New heavy isotopes of Rutherfordium (up to $^{267}$104) might be obtained in the $^{22}$O+$^{248}$Cm fusion reaction. The EvR cross sections in this reaction (shown in Fig. 16) are rather large and the beam intensity of $^{22}$O at the level of $10^8$ pps is sufficient to detect one decay event per week. Note that the reaction $^{22}$O+$^{248}$Cm is 3 MeV "colder" as compared to $^{18}$O+$^{248}$Cm ($E^*$(Bass) = 41 and 44 MeV, respectively) that allows one to measure even the 3n evaporation channel leading to $^{267}$104 (see Fig. 16). Half-lives of the heavy Rutherfordium isotopes (A>263) should be rather long to use chemical methods
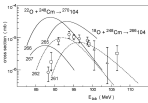
FIG. 16: Excitation functions for synthesis of Rutherfordium isotopes in the $^{18}$O+$^{248}$Cm (A=261 and A=262, dashed curves) and $^{22}$O+$^{248}$Cm (A=265, A=266 and A=267, solid curves) fusion reactions. Experimental data for the $^{248}$Cm($^{18}$O,5n)$^{261}$Rf reaction are from [31] (rectangles), [32] (triangles) and [33] (circles).

for their identification.



FIG. 17: Landscape of potential energy surface of the nuclear system formed in collision of $^{238}$U with $^{248}$Cm (contact configuration, dynamic deformation $\beta_2 = 0.2$, contour lines are drawn over 1 MeV energy interval). Open circles correspond to the most neutron-rich nuclei synthesized in $^{48}$Ca induced fusion reactions while the filled ones show SH nuclei produced in the "cold" fusion with lead target. The dotted line shows the most probable evolution in multi-nucleon transfer process.

## VII. MULTI-NUCLEON TRANSFER REACTIONS

The use of multi-nucleon transfer from heavy-ion projectile to an actinide target nucleus for the production of new nuclear species in the transuranium region has a long history. Light (carbon [34], oxygen and neon [35]), medium (calcium [36, 37], krypton and xenon [38, 39]) and very heavy ($^{238}$U [40, 41]) projectiles were used and heavy actinides (up to Mendelevium) have been produced in these reactions. The cross sections were found to decrease very rapidly with increasing transferred mass and atomic number of surviving target-like fragments. The level of 0.1 $\mu$b was reached for chemically separated Md isotopes [41].

These experiments seem to give not so great chances for production of new SH nuclei. However, there are experimental evidences that the nuclear shell structure may strongly influence the nucleon flow in the low-energy damped collisions of heavy ions. For example, in $^{238}$U-induced reactions on $^{110}$Pd at about 6 MeV/u bombarding energy an enhanced proton flow along the neutron shells $N_1 = 82$ and $N_2 = 126$ (reached almost simultaneously in target-like and projectile-like fragments) was observed in the distribution of binary reaction products [42].

The idea to take advantage of the shell effects for the production of SH nuclei in the multi-nucleon transfer processes of low-energy heavy ion collisions was proposed in [43]. The shell effects are known to play an important role in fusion of heavy ions with actinide targets driving the nuclear system to the quasi-fission channels (into the deep lead and tin valleys) and, thus, decreasing the
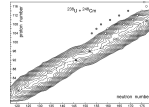
fusion probability. On the contrary, in the transfer reactions the same effects may lead to enhanced yield of SH nuclei. It may occur if one of heavy colliding nuclei, say $^{238}$U, gives away nucleons approaching to double magic $^{208}$Pb nucleus, whereas another one, say $^{248}$Cm, accepts these nucleons becoming superheavy in the exit channel – the so called "inverse" (anti-symmetrizing) quasi-fission process.

We extended our approach taking into consideration neutron and proton asymmetries separately instead of one mass-asymmetry parameter used before [11]. The potential energy surface of the giant nuclear system formed in collision of $^{238}$U and $^{248}$Cm nuclei is shown in Fig. 17. It is calculated within the two-center shell model for a configuration of two touching nuclei (with fixed value of dynamic deformation $\beta_2 = 0.2$) depending on numbers of transferred protons and neutrons. The initial configuration of $^{238}$U and $^{248}$Cm touching nuclei is shown by the crosses.

In low-energy damped collisions of heavy ions just the potential energy surface regulates to a great extent the evolution of the nuclear system. From Fig. 17 one sees that in the course of nucleon exchange the most probable path of the nuclear system formed by $^{238}$U and $^{248}$Cm lies along the line of stability with formation of SH nuclei which have many more neutrons as compared with those produced in the "cold" and "hot" fusion reactions. Due to fluctuations even more neutron rich isotopes of SH nuclei may be formed in such transfer reactions.

The yield of survived SH elements produced in the low-energy collisions of actinide nuclei is rather low, though the shell effects give us a definite gain as compared to a monotonous exponential decrease of the cross sec-
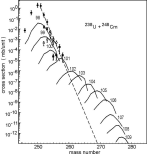
very high. In this connection more detailed experiments have to be performed aimed on the study of the shell effects in the mass transfer processes in low-energy damped collisions of heavy ions. The effect of "inverse" quasi-fission may be studied also in experiments with less heavy nuclei. For example, in the collision of $^{160}$Gd with $^{186}$W we may expect an enhanced yield of the binary reaction products in the regions of Ba and Pb just due to the shell effect [44]. The experimental observation of this effect and the measurement of the corresponding enhancement factor in the yield of closed shell nuclei might allow us to make better predictions (and/or simple extrapolations) for heavier nuclear combinations which are more difficult for experimental study.

## VIII. CONCLUSION

Thus we may conclude that there are several very promising possibilities for the synthesis of new SH elements and isotopes. First of all, we may use the titanium beam (instead of $^{48}$Ca) and actinide targets to move forward up to the element 120. The estimated EvR cross sections are rather low (at the level of 0.1 pb) but quite reachable at available setups. If the experiments with titanium beam will confirm our expectations, then we have to find a possibility to increase the beam intensity and the detection efficiency (totally by one order of magnitude) and go on to the chromium and iron beams (aiming to the elements 122 and 124). The use of light and medium mass neutron-rich radioactive beams may help us to explore and to fill the "blank spot" at the northeast part of the nuclear map. Such a possibility is also provided by the multi-nucleon transfer processes in low-energy damped collisions of heavy actinide nuclei, if the shell effects really play an important role in such reactions. The production of SH elements in fusion reactions with accelerated fission fragments looks less encouraging. Only if an extremely high beam intensity will be attained, the promises are increasing.



FIG. 18: Yield of survived isotopes of SH nuclei produced in collisions of $^{238}$U with $^{248}$Cm at 800 MeV center-of-mass energy. Experimental data for Cf (filled circles), Es (open rectangles), Fm (open circles) and Md isotopes (filled rectangles) obtained in [41] are also shown. Dashed line shows the expected locus of transfer reaction cross section without the shell effects.

tions with increasing number of transferred nucleons. In Fig. 18 the calculated EvR cross sections for production of SH nuclei in damped collisions of $^{238}$U with $^{248}$Cm at 800 MeV center-of-mass energy are shown along with available experimental data. As can be seen, really much more neutron rich isotopes of SH nuclei might be produced in such reactions.

Of course, the reliability of our predictions for the processes with a transfer of several tens of nucleons is not

[1] S. Hofmann and G. Münzenberg, Rev. Mod. Phys. **72**, 733 (2000).
[2] K. Morita et al., J. Phys. Soc. Jpn. **76**, No. 4, 043201 (2007); ibid. **76**, No. 4, 045001 (2007).
[3] Yuri Oganessian, J. Phys. G, **34**, R165 (2007).
[4] Yu.Ts. Oganessian, V.K. Utyonkov, Yu.V. Lobanov, F.Sh. Abdullin, A.N. Polyakov, R.N. Sagaidak, I.V. Shirokovsky, Yu.S. Tsyganov, A.A. Voinov, G.G. Gulbekian, S.L. Bogomolov, B.N. Gikal, A.N. Mezentsev, S. Iliev, V.G. Subbotin, A.M. Sukhov, K. Subotic, V.I. Zagrebaev, G.K. Vostokin, M.G. Itkis, K.J. Moody, J.B. Patin, D.A. Shaughnessy, M.A. Stoyer, N.J. Stoyer, P.A. Wilk, J.M. Kenneally, J.H. Landrum, J.F. Wild, and R.W. Lougheed, Phys. Rev. C **74**, 044602 (2006).
[5] V.I. Zagrebaev et al., NRV: Low Energy Nuclear Knowledge Base, http://nrv.jinr.ru/nrv.
[6] P. Möller, J. R. Nix, W. D. Myers, and W. J. Swiatecki, At. Data Nucl. Data Tables **59** (1995) 185.
[7] V.I. Zagrebaev, Y. Aritomo, M.G. Itkis, Yu.Ts. Oganessian, and M. Ohta, Phys. Rev. C **65**, 014607 (2002).
[8] V.I. Zagrebaev, Phys. Rev. C **64**, 034606 (2001).
[9] R.S. Naik, W. Loveland, P.H. Sprunger, A.M. Vinodkumar, D. Peterson, C.L. Jiang, S. Zhu, X. Tang, E.F. Moore, and P. Chowdhury, Phys. Rev. C **76**, 054604 (2007).
[10] V. Zagrebaev and W. Greiner, J. Phys. G **31**, 825 (2005).
[11] V. Zagrebaev and W. Greiner, J. Phys. G **34**, 1 (2007).
[12] U. Mosel, J. Maruhn, and W. Greiner, Phys. Lett. B **34**, 587 (1971); J. Maruhn and W. Greiner, Z. Phys. **251**, 431 (1972).
[13] V. Zagrebaev, A. Karpov, Y. Aritomo, M. Naumenko, and W. Greiner, Phys. Part. Nucl., **38**, No. 4, 469 (2007).

[14] V.I. Zagrebaev, AIP Conf. Proc. No. 704, 31 (2004).

[15] V.I. Zagrebaev, Nucl. Phys. **A734**, 164 (2004).

[16] R. Bass, *Nuclear Reactions with Heavy Ions* (Springer-Verlag, 1980), p.326.

[17] A.V. Yeremin, V.I. Chepigin, M.G. Itkis, A.P. Kabachenko, S.P. Korotkov, O.N. Malyshev, Yu.Ts. Oganessian, A.G. Popeko, J. Rohac, R.N. Sagaidak, M.L. Chelnokov, V.A. Gorshkov, A.Yu. Lavrentev, S. Hofmann, G. Munzenberg, M. Veselsky, S. Saro, K. Morita, N. Iwasa, S.I. Mulgin, and S.V. Zhdanov, JINR Report No. 6[92]-98, 1998.

[18] Zhao-Qing Feng, Gen-Ming Jin, Jun-Qing Li, and W. Scheid, Phys. Rev. C **76**, 044606 (2007).

[19] Z.H. Liu and Jing-Dong Bao, Phys. Rev. C **74**, 057602 (2006).

[20] T. Bürvenich, M. Bender, J.A. Maruhn, and P.-G. Reinhard, Phys. Rev. C **69**, 014307 (2004).

[21] K.-H. Schmidt and W. Morawek, Rep. Prog. Phys. **54**, 949 (1991).

[22] Yu.Ts. Oganessian, Phys. At. Nuclei, **69**, 932 (2006).

[23] Yu.Ts. Oganessian, V.K. Utyonkov, Yu.V. Lobanov, F.Sh. Abdullin, A.N. Polyakov, I.V. Shirokovsky, Yu.S. Tsyganov, G.G. Gulbekian, S.L. Bogomolov, B.N. Gikal, A.N. Mezentsev, S. Iliev, V.G. Subbotin, A.M. Sukhov, A.A. Voinov, G.V. Buklanov, K. Subotic, V.I. Zagrebaev, M.G. Itkis, J.B. Patin, K.J. Moody, J.F. Wild, M.A. Stoyer, N.J. Stoyer, D.A. Shaughnessy, J.M. Kenneally, P.A. Wilk, R.W. Lougheed, R.I. Il'kaev, and S.P. Vesnovskii, Phys. Rev. C **70**, 064609 (2004).

[24] V.I. Zagrebaev and W. Greiner, Nucl. Phys. **A787**, 363c (2007).

[25] K. Siwek-Wilczynska, I. Skwira-Chalot, and J. Wilczynski, Int. J. Mod. Phys. **E16**, 483 (2007).

[26] W.J. Swiatecki, K. Siwek-Wilczynska, and J. Wilczynski, Phys. Rev. C **71**, 014602 (2005).

[27] Yu.Ts. Oganessian, talk at the 3rd Int. Conf. TAN07, Davos, 2007.

[28] W. Loveland, Phys. Rev. C **76**, 014612 (2007).

[29] V.I. Zagrebaev, Phys. Rev. C **67**, 061601(R) (2003).

[30] V.I. Zagrebaev, V.V Samarin, and W. Greiner, Phys. Rev. C **75**, 035809 (2007).

[31] R.J. Silva, P.F. Dittner, M.L. Mallory, O.L. Keller, K. Eskola, P. Eskola, M. Nurmia, and A. Ghiorso, Nucl. Phys. **A216**, 97 (1973).

[32] R. Dressler, Ph.D. Thesis, University of Bern, 1999.

[33] Y. Nagame, M. Asai, H. Haba, S. Goto, K. Tsukada, I. Nishinaka, K. Nishio, S. Ichikawa, A. Toyoshima, K. Akiyama, H. Nakahara, M. Sakama, M. Schädel, J.V. Kratz, H.W. Gäggeler,f and A. Türler, J. Nucl. Rad. Sci. **3**, No. 1, 85 (2002).

[34] R.L. Hahn, P.F. Dittner, K.S. Toth, and O.L. Keller, Phys. Rev. C **10**, 1889 (1974).

[35] D. Lee, H. von Gunten, B. Jacak, M. Nurmia, Y.F. Liu, C. Luo, G.T. Seaborg, D.C. Hoffman, Phys. Rev. C **25**, 286 (1982).

[36] E.K. Hulet, R.W. Lougheed, J.F. Wild, J.H. Landrum, P.C. Stevenson, A. Ghiorso, J.M. Nitschke, R.J. Otto, D.J. Morrissey, P.A. Baisden, B.F. Gavin, D. Lee, R.J. Silva, M.M. Fowler, and G.T. Seaborg, Phys. Rev. Lett. **39**, 385 (1977).

[37] A. Türler, H.R. von Gunten, J.D. Leyba, D.C. Hoffman, D.M. Lee, K.E. Gregorich, D.A. Bennett, R.M. Chasteler, C.M. Gannett, H.L. Hall, R.A. Henderson, and M.J. Nurmia, Phys. Rev. C **46**, 1364 (1992).

[38] K.J. Moody, D. Lee, R.B. Welch, K.E. Gregorich, G.T. Seaborg, R.W. Lougheed, and E.K. Hulet, Phys. Rev. C **33**, 1315 (1986).

[39] R.B. Welch, K.J. Moody, K.E. Gregorich, D. Lee, G.T. Seaborg, Phys. Rev. C **35**, 204 (1987).

[40] M. Schädel, J.V. Kratz, H. Ahrens, W.Brüchle, G. Franz, H. Gäggeler, I. Warnecke, G. Wirth, G. Herrmann, N. Trautmann, and M. Weis, Phys. Rev. Lett. **41**, 469 (1978).

[41] M. Schädel, W. Brüchle, H. Gäggeler, J.V. Kratz, K. Sümmerer, G. Wirth, G. Herrmann, R. Stakemann, G. Tittel, N. Trautmann, J.M. Nitschke, E.K. Hulet, R.W. Lougheed, R.L. Hahn, and R.L. Ferguson, Phys. Rev. Lett. **48**, 852 (1982).

[42] W. Mayer, G. Beier, J. Friese, W. Henning, P. Kienle, H.J. Körner, W.A. Mayer, L. Müller, G. Rosner, W. Wagner, Phys. Lett. B **152**, 162 (1985).

[43] V.I. Zagrebaev, Yu.Ts. Oganessian, M.G. Itkis, and W. Greiner, Phys. Rev. C **73**, 031602(R) (2006).

[44] V. Zagrebaev and W. Greiner, J. Phys. G **34**, 2265 (2007).